Measuring the Area and Number of Ballast Particle Contacts at Sleeper/Ballast and Ballast/Subgrade Interfaces

T. Abadi[1], L. Le Pen[1], A. Zervos[1], and W. Powrie[1]

[1]Infrastructure Research Group, University of Southampton; United Kingdom

Abstract

The number of railway ballast particles in contact with a sleeper may be relatively small. The discrete and non-uniform nature of these contacts may cause breakage and wear. This article explores the use of pressure paper to record the loading history of sleeper to ballast particle contacts over >3 million loading cycles in full size tests. The results demonstrate that the actual contact area may be less than 1% of the total, and that the number of individual contacts is in the hundreds. Under sleeper pads, a finer ballast grading, a shallower shoulder slope and changes to the sleeper material are found to increase the number and area of contacts.

Keywords: ballast, sleeper, pressure paper, under sleeper pad (USP), grading.

1 Introduction

In track bed design, the pressure distribution beneath the sleeper is commonly idealized as a "ω" shaped distribution (Figure 1, see e.g. [1] for a summary). For the purposes of evaluating the maximum contact pressure transferred to the ballast the ω shaped pressure distribution may then be transformed to two equivalent area rectangles (as described by [2]) beneath each railseat using an approximation such as equation 1 [3].

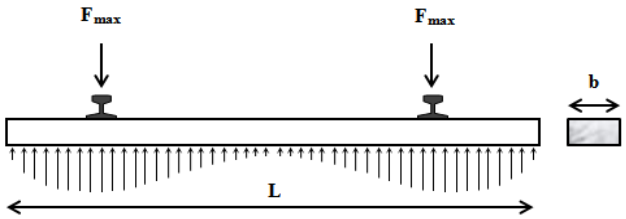

Figure 1: Typical idealised pressure distribution along the sleeper (after [3])

$$\frac{3\,F_{max}}{b\,L} = \sigma_{max} \quad (1)$$

Where F_{max} is the maximum railseat load per rail including any dynamic factor if appropriate and b and L are the sleeper length and width respectively assuming a single rectangular based sleeper (mono-block). The multiplier 3 comes from assuming that 2/3 of the sleeper length (1/3 of the sleeper length per rail) is loaded by the equivalent rectangular pressure distributions. For a 5 tonne railseat load this implies a maximum contact pressure of 210kPa for a G44 concrete mono-block sleeper of dimensions 2.5 m (L) × 0.285 m (b) [4].

While this idealisation can be useful, the load transfer behaviour at the sleeper/ballast interface is highly variable both within and between individual sleepers and may also vary with cycles of loading. This is a result of the relatively large particle sizes of ballast in relation to a typical sleeper footprint and varying rates of plastic settlement of the ballast with loading cycles. This variability was apparent in measurements using pressure cells mounted along the sleeper base carried out by British Rail Research [5] in the 1970s. Figure 2 shows that for the same railseat load, when the pressure is averaged over a smaller local area equivalent to the size of the measuring pressure plate the maximum contact pressure is slightly higher than the idealisation of equation 1 at nearly 300kPa. The size of the pressure plates used to produce Figure 2 was not reported, although it may be inferred from the changes in direction of the line of best fit that these were of the order of 100 mm. [5] also estimated that the number of particles in contact with the sleeper was between 100 and 200.

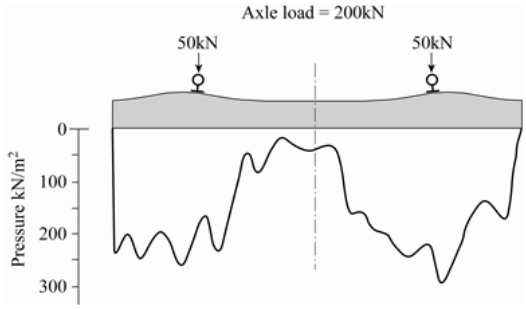

Figure 2: Sleeper base contact pressure distribution (after [5])

The approximation of Equation 1 and the measurements by British Rail assume that the variations in pressures can be characterised by averaging over contact areas that are large in relation to individual particle contact areas. As will be shown this is an assumption that increasingly breaks down as the area of interest approaches the area of interaction between individual particle/sleeper contacts.

In this paper, the feasibility of using pressure paper to investigate sleeper to ballast and ballast to sub-grade contact areas and stresses at the scale of individual particles is demonstrated. The effect on the pattern and number of contacts of the sleeper type, ballast grading, and modification of the sleeper/ballast interface through the provision of an under-sleeper pad is then assessed. The number of contacts for each arrangement is then compared to the number of contacts potentially available for a given grading based upon a simplified methodology.

2 Methods

2.1 General

The Southampton Railway Testing Facility (SRTF) is used to investigate the response of different combinations of sleepers and ballast to cyclic loading, over millions of load cycles representative of axle loads in Europe and elsewhere. The SRTF comprises two vertical sides 5 m long and 0.65 m high, constructed from heavy steel sections and panels. Wooden and steel panels of 500 mm by 650 mm are firmly attached on the inside walls of the SRTF apparatus and covered by a double layer of plastic sheet to minimise friction at the contact with the ballast. The walls are held at a fixed distance of 0.65 m apart, corresponding to a typical UK sleeper spacing. The test bay maintains conditions as close to plane strain as practicable. A fuller description of the apparatus can be found in [6 & 7]. Figures 3 and 4 show a plan and two photos of the SRTF in the laboratory.

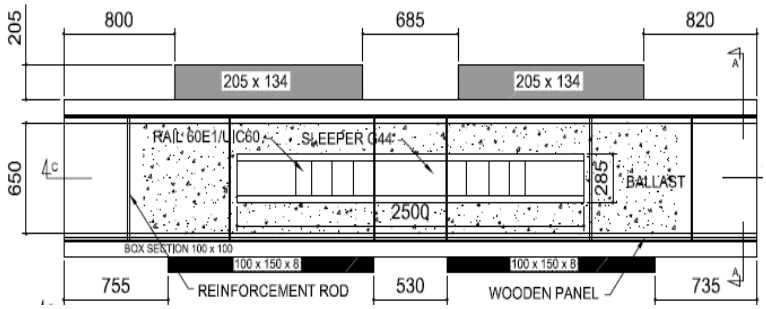

Figure 3: Plan view of the SRTF

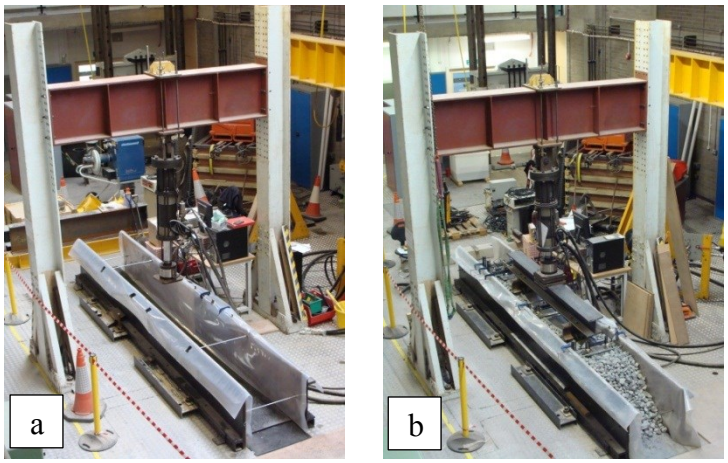

Figure 4: The SRTF (a) empty and (b) ready for a test

Figure 5 shows a cross section of the test set-up. At the base of the ballast bed a substrate consisting of a rubber mat 12 mm thick was used to represent a slightly compressible subgrade. Its thickness was chosen so that the cyclic deflection of the sleeper reached realistic values (up to 1 mm) during testing.

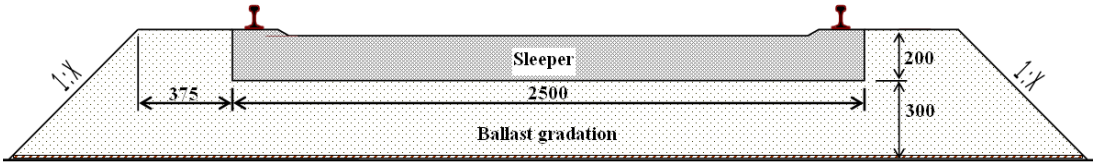

Figure 5: Test cross-section through a typical test set-up

Procedures followed in all tests were as follows:

1. The ballast was placed to the full width and 300 mm depth up to the level of the sleeper base and compacted with a total of 22 passes of a 22 kg, 400 mm × 320 mm plate vibrator with a 5kN compaction force, and the surface levelled at the same time.
2. The sleeper was placed on top of the ballast. The crib ballast was placed and the shoulder ballast surface was raised to the same level as the sleeper surface. Usually the shoulder slope was 1V:1H but one had a slope of 1V:2H.
3. A loading beam was placed across the railheads and aligned with the connection to the hydraulic actuator.
4. A load of 5kN was applied and increased to 98.1kN at a slow rate (5kN/s) to bed the sleeper in and confirm that the connection was stable enough for subsequent 3Hz cyclic loading. The load was held at 98.1kN for approximately 2 minutes then reduced to 5kN.
5. Cyclic loading was then applied using a sinusoidal load form at a frequency of 3Hz between 5kN and 98.1kN
6. At the end of each test, all materials were removed from the SRTF apparatus including the ballast. Fresh ballast was used in each test to ensure repeatability of initial conditions.

The loading was intended to represent a 20 tonne axle load assuming a 50% load transfer to the sleeper immediately beneath the wheel (i.e. 98.1kN). That this is a reasonable assumption can be demonstrated by means of a beam on elastic foundation analysis [8 & 9] with typical rail and track support stiffnesses. 20 tonnes is greater than most passenger train axle loads and slightly below the maximum permitted freight axle load in the UK (22.5 tonnes).

The loading rate of 3Hz enabled the tests to be carried out within a reasonable timescale (e.g. 12 days for 3 million cycles) while maintaining pseudo-static loading regime (i.e. accelerations did not become significant compared with gravity).

2.2 Pressure paper

Pressure paper is a thin film consisting of micro-encapsulated colour forming and colour developing materials [10]. Its properties are described in detail by Fuji Film [11]. The pressure paper turns red when subjected to a pressure, with the intensity of the colour proportional to the magnitude of the pressure. The papers used in these tests were tested to confirm their properties prior to use (described later). In this research, pressure paper with stated sensitivities in the ranges 2.5 to 10MPa, and 10

to 50MPa were used. Sheets of the pressure paper measuring 200 mm × 250 mm were placed at key locations on the rubber mat substrate and at the sleeper soffit in each test to measure the interface of sleeper/ballast and ballast subgrade respectively (Figure 6 and Table 1). In the tests reported here the pressure paper was left in place for the entire test. It therefore provided a cumulative record of the contact positions and the maximum local pressures over the whole of the loading history, and this must be borne in mind when interpreting the results.

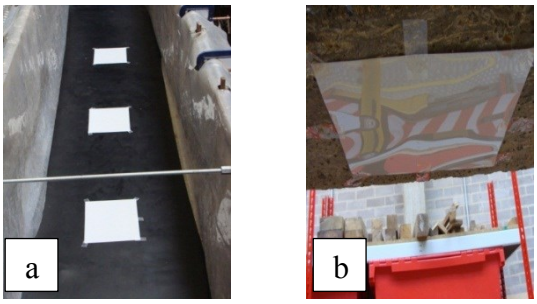

Figure 6: Pressure paper location (a) on the rubber mat and (b) at the sleeper soffit

Interface	Sheets	Location details	Sensitivity
sleeper/ballast	3	One below the middle and one directly under each railseat.	10 to 50MPa
ballast/substrate	3	Directly below each of the sheets attached to the sleeper soffit	2.5 to 10MPa and 10 to 50MPa

Table 1: Pressure paper locations

To verify the relationship between colour intensity and pressure, calibration checks were carried out in which a known weight was placed on the pressure paper to apply uniform pressure over a 2 minute duration. The red patches produced were scanned after a range of elapsed times (up to three months) following loading to evaluate the influence of time on the red intensity (RI) present because the red intensity fades with time [12]. After 3 months the RI associated with a given pressure may be ~10% lower than immediately after loading. A bespoke script implemented in Matlab [13] was used to determine this reduction so that it could be allowed for. However, in this paper the pressure analysis is not reported as the focus of this paper is on determining the location and area of contacts. To this end it was found that the locations of contacts could be reliably recorded through selection of paper in an appropriate sensitivity range based on the probable range of pressures likely to be encountered. It was found that the paper rated 10MPa to 50MPa was suitable for placement beneath the sleeper, whereas a double layer of papers rated from 2.5MPa to 10MPa and 10 to 50MPa was more suitable for use at the ballast base. The calibration tests carried out for this research (in which known pressures were applied to the pressure paper and the RI measured) demonstrated that:

- The paper stated by the manufacturer to be sensitive between 10 to 50MPa can provide data to as low as 2.5MPa.
- The paper with a stated sensitivity range of 2.5 to 10MPa provides data to as low as 0.5MPa.

- Where stresses exceed the maximum sensitivity of the paper the paper remained red to its maximum RI and provided a record of contact at the location.

Section 3 describes the different sleeper types and materials tested.

3 Materials and theory

3.1 Sleeper

Several different types of sleeper were tested to investigate the influence of sleeper material and geometry. Mono-block sleepers made of concrete, plastic, and timber were tested together with a twin-block sleeper made of concrete. The characteristic sleeper dimensions are given in Table 2.

Type of sleeper	Dimension of sleeper (m)			Soffit area (m^2)
	Width	Height	Length	
Mono-block G44	0.285	0.200	2.500	0.713
Plastic	0.250	0.150	2.600	0.650
Timber	0.250	0.130	2.600	0.650
Twin-block B450	0.295	0.245	2.415	0.496

Table 2: Dimensions and types of sleepers tested

3.2 Ballast

Crushed granite rock was sourced from Cliffe Hill quarry, Leicestershire, U.K. Cliffe Hill quarry provides aggregates that meet Network Rail (NR) ballast requirements [14] and industry standard aggregate grading specifications [15]. To investigate the influence of varying the grading (particle size distribution), three variant ballast gradings were prepared and tested with a G44 mono-block concrete sleeper.

The intention of varying the ballast grading was to introduce a higher proportion of finer (gravel sized) material to the regular ballast grading on the basis that this could increase the number of contact points between the sleeper and the ballast and reduce contact stresses, thereby extending the life of the ballast and sleeper and reducing the susceptibility to settlement. However, there are some practical restrictions on the type of grading that can be used. In particular, the requirement to maintain a minimum hydraulic conductivity in the presence of fouling material [16 & 17] has meant that ballast gradings around the world tend to be very uniform with particles in a narrow size range, from 20 mm to 65 mm. Indraratna and Salim [18] investigated ballast gradings and suggested that a new better performing ballast grading that would maintain an acceptable hydraulic conductivity should have a uniformity coefficient (C_u) in the range $2.2 \leq C_u \leq 2.6$, where C_u is defined as:

$$C_u = \frac{D_{60}}{D_{10}} \tag{2}$$

Where D is the particle diameter (sieve size aperture) and the subscript denotes the percentage of particles smaller than by mass. These values can be read from a standard particle size distribution plot (e.g. Figure 7). In comparison Network Rail ballast has a substantially lower uniformity coefficient of 1.5. The particle size distribution (PSD) curves for each ballast grading tested are shown in Figure 7. Values of C_u are given in Table 3, together with key particle diameters and data for 10-20 aggregate (explained later).

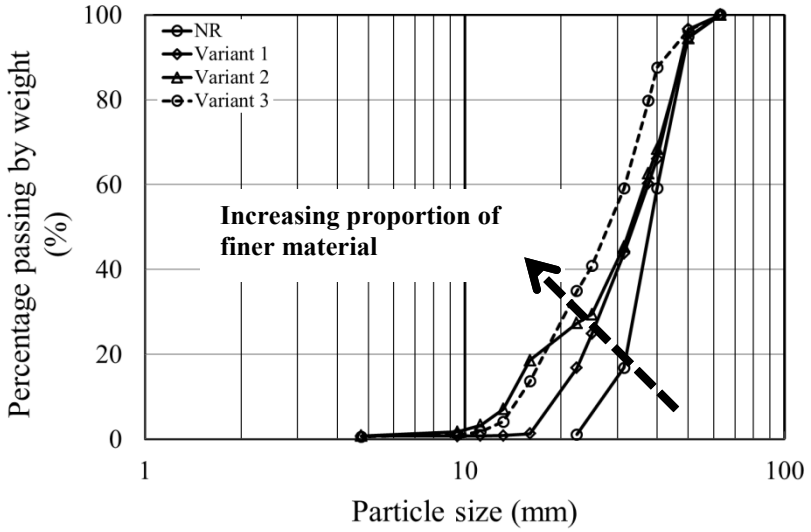

Figure 7: PSD comparison of variant and Network rail (NR) standard gradings

Grading	Particle size (mm)						
	D_{10}	D_{50}	D_{60}	D_{70}	D_{90}	D_{100}	C_u
NR	27.6	38.0	40.0	43.2	49.1	63.0	1.5
Variant 1	19.5	33.9	37.7	41.5	47.5	63.0	1.9
Variant 2	14.7	33.1	36.9	41.0	48.5	63.0	2.5
Variant 3	15.5	27.2	30.0	34.2	47.5	63.0	1.9
10/20 (Stoneblower)	12.1	16.0	16.71	17.86	20.7	22.9	1.4

Table 3: Key data for NR ballast and modified gradings

A further intention in designing the variant ballast gradings was to maintain as closely as possible a linear distribution on the log scale while fixing the maximum size of D_{90} close to the existing value for NR ballast of about 49 mm. By making some simplifying assumptions it is possible to gain some insights into how having a distribution that is linear on a log PSD plot influences the density of the packing achievable and to estimate the number of potential contacts available at a bounding surface. To calculate the number of contacts potentially available a method is developed as follows:

Assume that the PSD distribution is linear on a log scale between D_{10} and D_{90} e.g.as shown in Figure 8 (a).

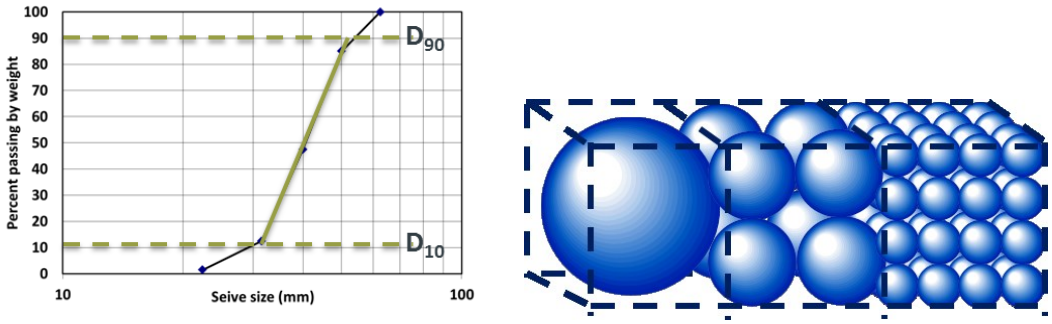

Figure 8: (a) Idealised PSD, (b) visualisation of sleeper/particle contact with discrete sizes in log distribution for two particle sizes

Therefore:

$$\% \text{ passing} = m.\ln(D_n) + C \tag{3}$$

It can then be shown that the ratio of particles of size D_A to D_B (where there are equivalent mass fractions of each particle size) potentially in contact with a flat surface assuming square packing is found from:

$$\sqrt[\frac{2}{3}]{\frac{1}{D_A^3}} : \sqrt[\frac{2}{3}]{\frac{1}{D_B^3}} \tag{4}$$

This is shown visually in Figure 8(b) for three particle sizes and can be described thus; one large particle providing one contact is equivalent in mass to 8 particles of half the size (though these only provide 4 contacts) and 64 particles of one quarter of the size (though these only provide 16 contacts). Hence each side of equation (4) is built up from the need to:
(1) invert the cube of the particle size to obtain the number of particles per unit volume [the 1, 8 or 64 in Figure 8(b)],
(2) take the cube root of the resulting value to obtain the number of particles per unit length [1, 2 or 4 in Figure 8b]
(3) square this result to obtain the number of particles per unit area (the 1, 4 or 16 in Figure 8b).
The ratio expressed in (4) can be used to develop an equation to estimate the number of contacts against a flat surface provided the overall PSD is linear on a log scale and can be characterized by a ***discrete*** number of particle sizes. If this criteria is met then the "potential" number in contact with a flat bounding surface $\mathbf{C_p}$ can be determined using the formula:

$$C_P = \left(\frac{A_{sleeper}}{N.D_A^2}\right) \cdot \left(\frac{\sqrt[\frac{2}{3}]{\frac{1}{D_A^3}} + \sqrt[\frac{2}{3}]{\frac{1}{D_B^3}} + \ldots \sqrt[\frac{2}{3}]{\frac{1}{D_N^3}}}{\sqrt[\frac{2}{3}]{\frac{1}{D_A^3}}:}\right) \tag{5}$$

Where N is the number of discrete particle sizes evaluated (where the mass of particles in each size fraction is equivalent), D_A to D_N are the particle diameters for

each size fraction and $A_{sleeper}$ is the contact area of the base of the sleeper. The first bracketed term on the right hand side of Equation (5) determines the number of the largest size fraction particles (D_A) in contact with the 1/N proportion of the sleeper soffit area, the second bracketed term sums the ratio of D_A sized particles to the remaining size fractions D_B to D_N, by multiplying these two terms together the total number of contacts is obtained. Equation (5) can be applied to any log linear PSD distribution where m and C are known and D_A to D_N can be determined by manipulation of equation 3. However, it is perhaps simpler to read the particle sizes from a PSD graph such as Figure 8(a). This simplified method to calculate an estimate of the potentially available ballast to sleeper contacts will be used later as a comparison with those measured using the pressure paper.

3.3 Under sleeper pad

Under sleeper pads (USPs) for improved track performance (as opposed to noise reduction) are a relatively recent development, and while the mechanisms of behaviour are not fully understood such USPs are generally considered to protect the ballast, reduce ballast and sleeper wear and help prevent rail corrugation [19 & 20]. To explore how performance USPs alter the sleeper/ballast interface, two types of pad were tested having the properties shown in Table 4.

Property	USP1	USP2
Technical ID	FC500	FC208GF
Thickness	4 mm	9 mm
Weight	6 kg/m^2	5.6 kg/m^2
Stiffness (C_{Stat})	0.228-0.311 N/mm^3	0.079-0.105 N/mm^3
Core (inner) material	Trackelast FC500	Bonded cork

Table 4: Properties of USPs tested (after [21])

USP 1 comprised a blend of thermoplastic materials and elastomeric inclusions while USP 2 was made of a high quality cellular rubber bonded cork.

Using the stiffness-based classification criteria proposed by Auer et al. [22], USP1 and USP2 would be categorised as "stiff" (0.25 N/mm^3 $\leq C_{Stat} \leq$ 0.35 N/mm^3) and "soft" (0.10 N/mm^3 $\leq C_{Stat} \leq$ 0.15 N/mm^3) respectively. These USPs were tested with concrete mono-block G44 type [4] and concrete twin-block B450 type sleepers [23]. It is possible to cast these USPs into the sleepers during manufacture, but for the current tests the USPs were glued to the sleeper soffits using epoxy adhesive.

3.4 Other modifications tested

Anderson and Key [24] tested a two layered ballast (TLB) system to explore the effect on performance of a layer of smaller aggregates placed immediately beneath the sleeper. This was intended to represent the effect of maintenance by stone blowing [25 & 26], in which smaller sized particles (10 mm to 20 mm) are "blown" beneath the railseats to restore track level and smooth out short wavelength faults.

Stone blowing is an alternative maintenance practice to tamping although it is usually employed only after tamping has become ineffective and is not widely used outside the UK. Claisse et al [27] and Claisse and Calla [28] investigated whether placing smaller sized aggregate in the crib could provide a reservoir of material that would fill any ballast voids under sleepers that may occur due to cyclic loading. However, smaller aggregates at the surface can be susceptible to the phenomenon of ballast flight [29]. In this research a modified form of two layer ballast system was simulated in which a 50 mm thick layer of finer, 10-20 mm particles (as used in stone blowing) was placed beneath the sleeper and protected from ballast flight by a covering of regular ballast within the crib and on the shoulder. The overall geometry was the same as in the other tests, with the 50 mm layer of 10-20 mm aggregate underlain by a 250 mm thickness of regular ballast to create a total ballast depth below the sleeper soffit of 300 mm.

Figure 9 shows the PSDs of the standard and 10-20 mm materials used (see also Table 3). Figure 10 shows photographs taken during construction illustrating the top of the 10-20 mm layer level with the sleeper soffit and the final form following placement of the topmost layer of regular ballast.

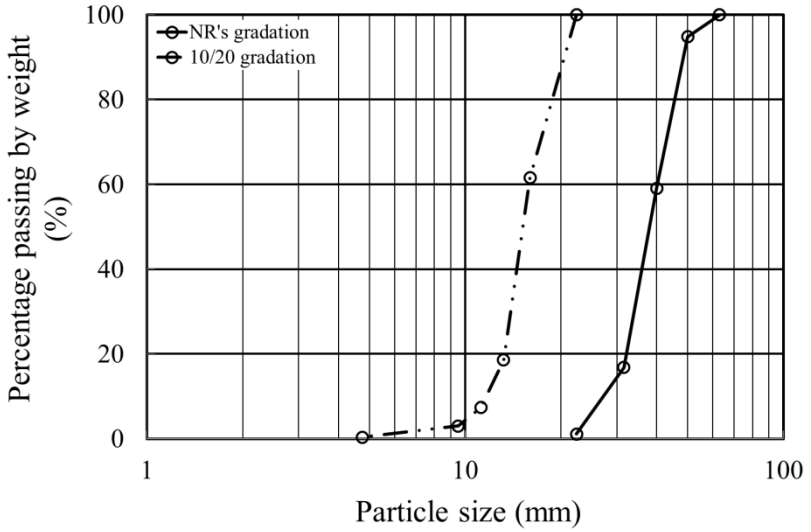

Figure 9: PSD graphs for NR and 10-20 mm gradings used in the system

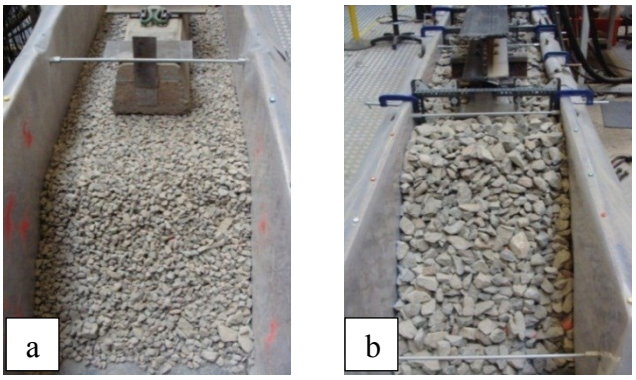

Figure 10: TLB under construction: (a) the upper surface of the 10-20 mm material, and (b) following placement of the final covering of regular ballast

A final consideration was the slope of the ballast shoulder away from the tracks. The ballast shoulder plays an important part in preventing lateral movement of the track [7], but it appears that there is no international consensus regarding the optimum shoulder slope. In Germany a 1V:1.25H shoulder slope has been recommended [30], while in Australia a shallower slope of 1V:1.5H has been applied by most railway authorities (e.g. [31]). USA [32] and UIC [33] standards recommend a slope of 1V:2H. In the UK, there is apparently no standard and space constraints mean that in many cases the ballast stands at its natural angle of repose with a slope of approximately 1V:1H, which was adopted as the standard in the current series of tests. To investigate the effect of the shoulder slope on the lateral restraint offered to the track, a test with re-profiled shoulder slopes of 1V:2H constructed from standard ballast with a mono-block concrete G44 sleeper was carried out.

4 Test details

In total twelve tests are reported. All tests were carried out to at least 3 million load cycles with some tests continued to up to 6 million load cycles (Table 5). The grade of pressure paper used in what was intended to be the baseline test on a concrete mono-block sleeper with standard NR ballast was subsequently found to have an unsuitable pressure range. Thus for comparative purposes the test on a concrete mono-block sleeper with ballast grading variant 1 is often referred to. This is considered an acceptable approximation because the performance of this ballast grading was found to be almost identical to NR standard ballast in terms of stiffness and overall plastic settlement [34]. Also the relatively small quantity of finer material used in variant 1 meant that the grading remained close to the current NR standard (Table 3) and should provide approximately the same number of potential contacts estimated by Equation (5) (values given later).

Test ID	Parameters			Total load cycles (Millions)
	Ballast	Sleeper	USP	
Variant 1 (close to NR)	Variant 1	G44	No	3.0
Plastic	NR	Plastic	No	4.0
Timber	NR	Timber	No	3.5
Variant 2	Variant 2	G44	No	3.0
Variant 3	Variant 3	G44	No	5.0
TLB (Two Layer Ballast)	TLB	G44	No	4.0
RPS (Re-profiled Shoulder)	NR	G44	No	3.5
Mono-block + USP 1	NR	G44	1	3.0
Mono-block + USP 2	NR	G44	2	4.0
Twin-block (NR)	NR	Twin	No	4.5
Twin-block + USP 1	NR	Twin	1	4.5
Twin-block + USP 2	NR	Twin	2	6.0

Table 5: Summary of tests reported

5 Results

The pressure paper was recovered at the end of each test and the contact regions analysed in terms of number, area and where possible level of stress present.

5.1 Sleeper/ballast interface

Figures 11-16 show the contacts recorded by pressure paper located at the sleeper soffit for mono-block sleepers made of different materials (Figure 11), an increase in the amount of finer material in the ballast (Figure 12), the modified two layer ballast system (Figure 13), a re-profiled ballast shoulder slope (Figure 14) and the presence of under sleeper pads on mono-block (Figure 15) and twin-block sleepers (Figure 16). In the Figures where the sleepers are mono-block variant 1 is shown for comparison as this is the closest to NR ballast available. For the twin-block tests an NR ballast test is shown for comparison

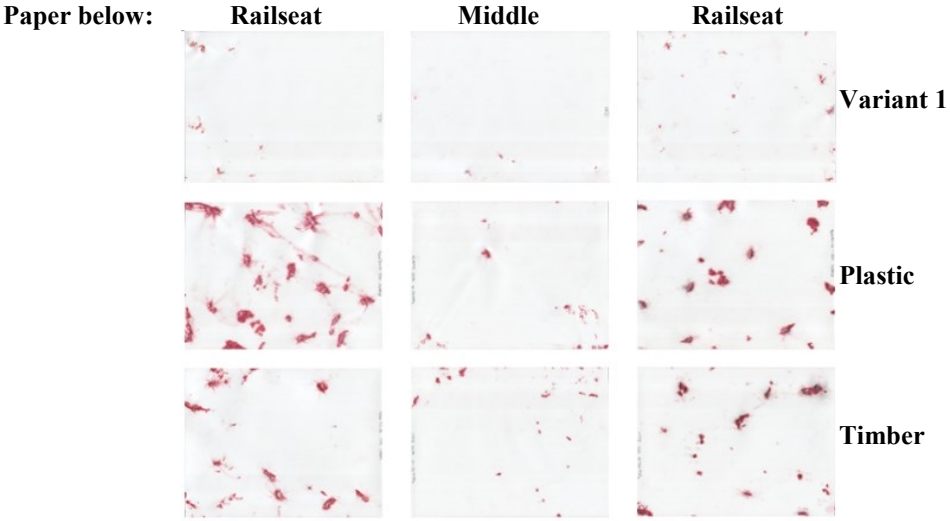

Figure 11: Particle contact histories at the sleeper/ ballast interface: mono-block sleeper, effect of sleeper material

In Figure 11 it can be seen that the contacts beneath the railseats are more pronounced. This can be explained as a result of particles nearer the sleeper ends being more easily displaced owing to the relatively lower confinement compared to the sleeper middle. The larger red marks therefore represent a merging of all the contact locations of individual particles that have moved around. It is also worth noting that in general these larger marks are later counted as individual contact locations. Figure 11 also confirms that the softer sleeper materials (plastic and timber) produced larger contact areas per particle. Figure 12 shows that as the finer proportion increases the number of contacts increases. In Figure 13 the contacts are more numerous and appear more uniformly distributed for the TLB test which had the finest grading.

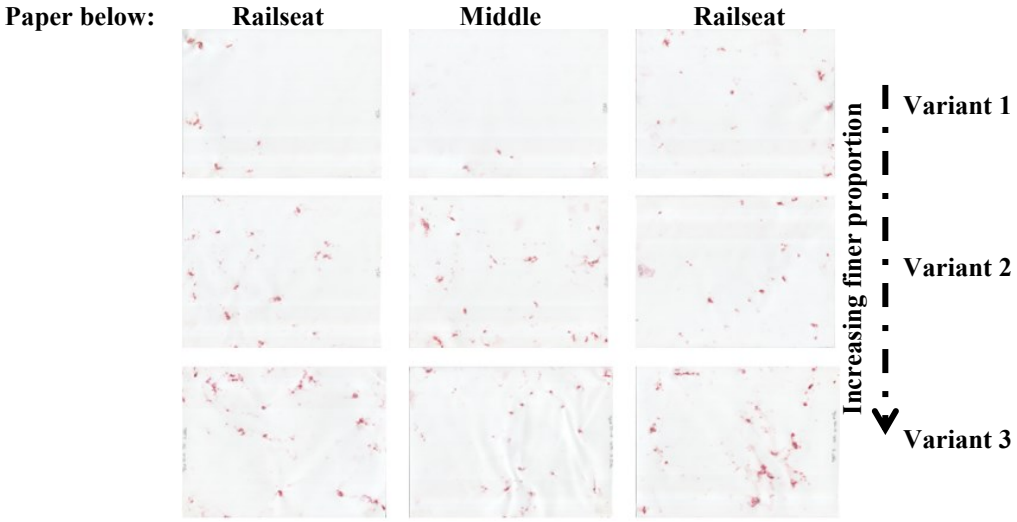

Figure 12: Particle contact histories at the sleeper/ ballast interface: mono-block concrete sleeper, effect of increasing the proportion of fine material in the ballast

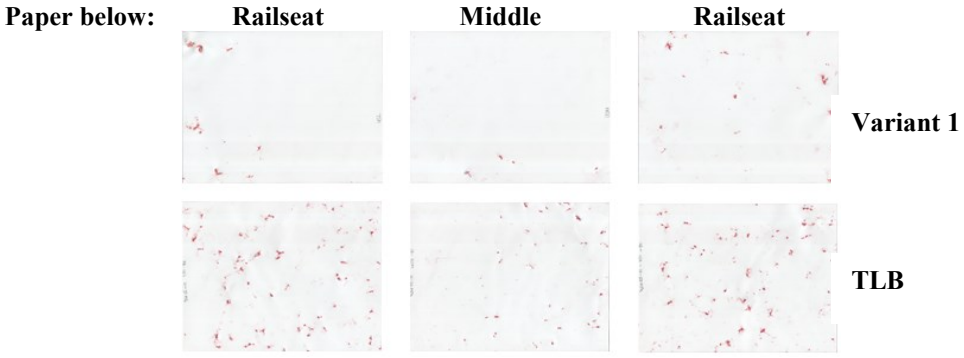

Figure 13: Particle contact histories at the sleeper/ballast interface: mono-block concrete sleeper, effect of a modified two-layer ballast system

Figure 14 shows that more contacts are present in the re-profiled shoulder (RPS) test, although many of these are small and difficult to distinguish. For the bottom left image in Figure 15 there was some blue colour distortion around the edge of this piece of paper caused by moisture from the ballast which was not completely dry when it was placed into the SRTF. However this blue distortion did not interfere with the red intensity data. Also, for the paper in the stiff USP test in Figure 15 below the right railseat some particles appear to have moved more significantly than usual over the 3 million cycles of the test. This has resulted in more marking on the paper giving the impression of a larger contact area. For the tests in which USPs were fitted to both mono-block and twin-block concrete sleepers (Figures 15 & 16) individual particle contacts were clearly present over larger areas than for the same sleeper without the USP.

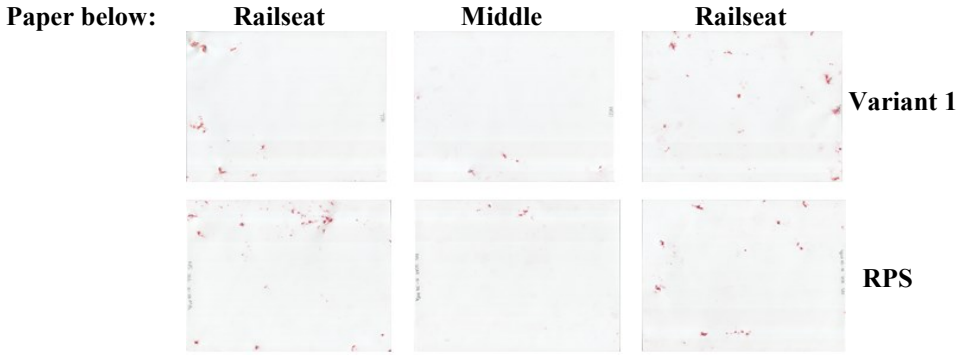

Figure 14: Particle contact histories at the sleeper/ballast interface: mono-block concrete sleeper, effect of a re-profiled shoulder (RPS) slope

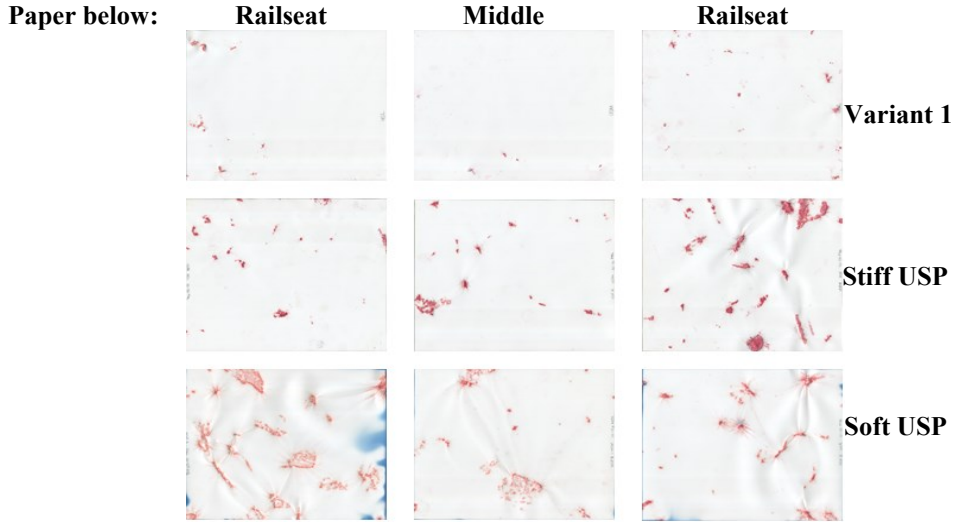

Figure 15: Particle contact histories at the sleeper/ballast interface: mono-block concrete sleeper, effect of under sleeper pads

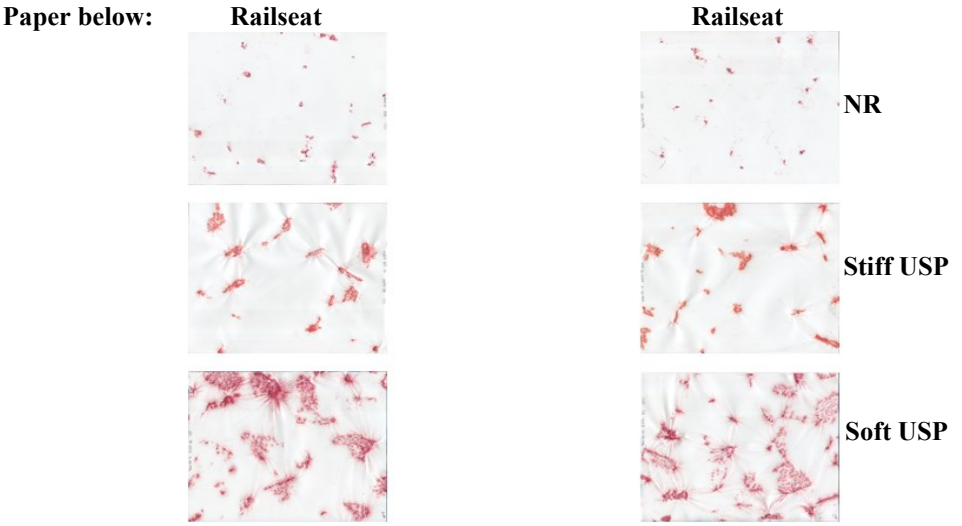

Figure 16: Particle contact histories at the sleeper/ballast interface: duo-block concrete sleeper, effect of under sleeper pads

The number of contact points was counted manually, by the same person in each case, while the total contact area was determined by thresholding and segmenting the images at the same cut-off values using Adobe Photoshop CS2 software. Cyclic loading abraded and wore through the paper at a small number of less stable particle/sleeper contacts, which moved about from cycle to cycle. These abraded locations were surrounded by red from the bordering intact paper so the historical contact area could still be determined using a hole filling function within the analysis software used. This data is summarised in Table 6.

Sleeper type	Test ID	Notes	Number of contacts per sleeper, 10-50MPa pressure paper	Percentage contact area per sleeper, 10-50MPa pressure paper	Average contact pressure, MPa calculated as $F_{max}/A_{contact}$
Mono-block	Variant 1		147	0.18	76.5
	Plastic	NR	360	3.08	4.9
	Timber		420	1.56	9.7
	Variant 2	↓ Increasing finer proportion	347	0.38	36.2
	Variant 3		836	0.63	21.9
	TLB	Two layered	1311	0.52	26.5
	RPS	NR	451	0.2	68.8
	+ USP 1	Stiff	314	1.64	8.4
	+ USP 2	Soft	447	1.05	13.1
Twin-block	Baseline	NR	243	0.53	32.3
	+ USP 1	Stiff	268	2.91	5.9
	+ USP 2	Soft	329	4.75	3.6

Table 6: The number and area of particle contacts at the ballast/sleeper interface in each test, and the implied average contact pressure

The numbers of contacts for the whole sleeper given in Table 6 have been calculated by summing the number of contacts for all pieces of contact paper present in each test and then multiplying by the ratio of paper area to sleeper soffit area.

The percentage contact area in Column 5 is the percentage of red area over the pressure paper present in each test. Given that the areas of red were not necessarily all under pressure at the same time, this is likely to be an overestimate of the actual area of contact at any given time. A further approximation is introduced by the assumption that the proportions of contact area are the same over the pressure paper and over the sleeper as a whole. Although the pressure determined by RI analysis of the pressure paper is not reported here, an estimate of the apparent contact pressure may be made by dividing the maximum applied load by the contact area and this is shown in column 6. It can be seen that these average contact pressures based upon the measured area of sleeper/ballast contacts are many times greater than those

estimated using the AREMA approximation of Equation 1, which gives 210kPa for a mono-block G44 sleeper.

5.2 At the base of the ballast layer

Figures 17-22 show the pressure paper sheets placed at the base of the ballast layer, after each test.

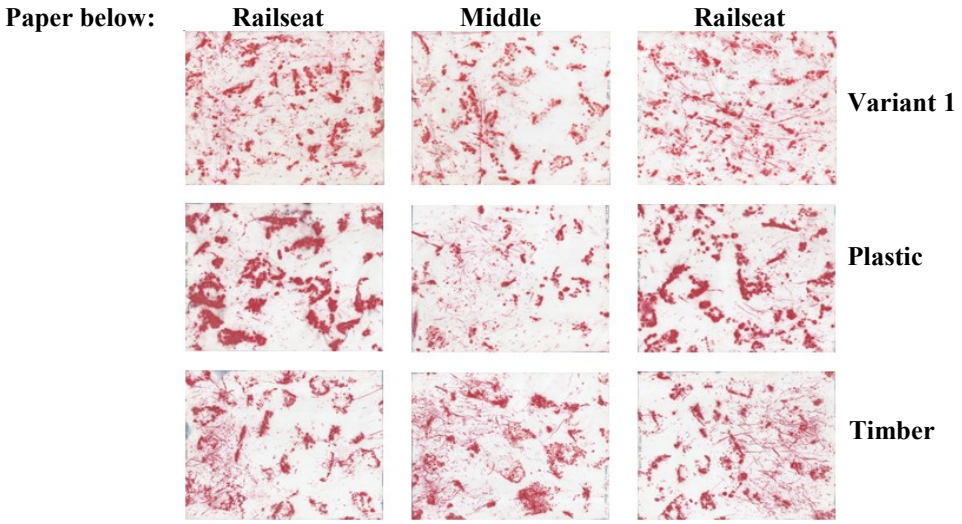

Figure 17: Contact areas recorded at the ballast/subgrade interface: mono-block sleepers made of different materials

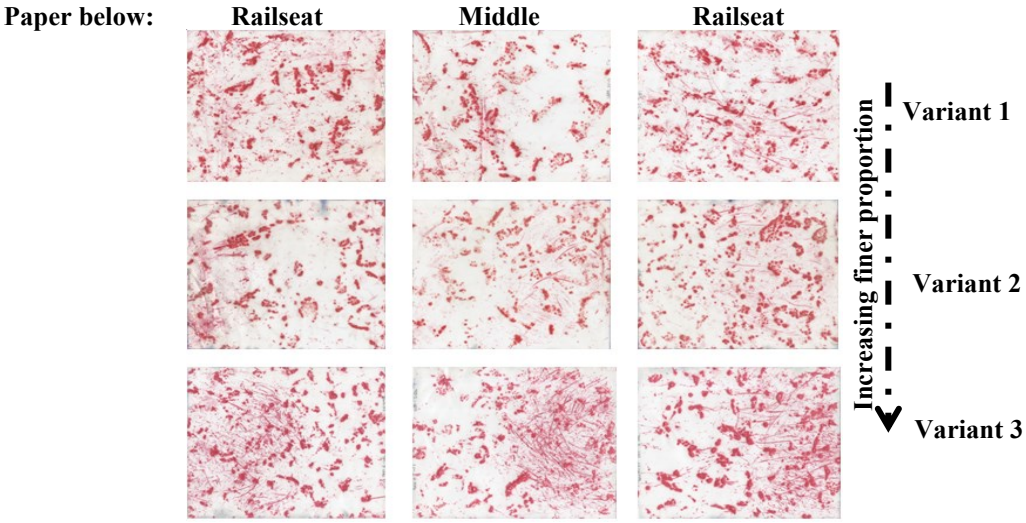

Figure 18: Contact areas recorded at the ballast/subgrade interface: mono-block concrete sleepers and effect of increasing the finer material in the ballast

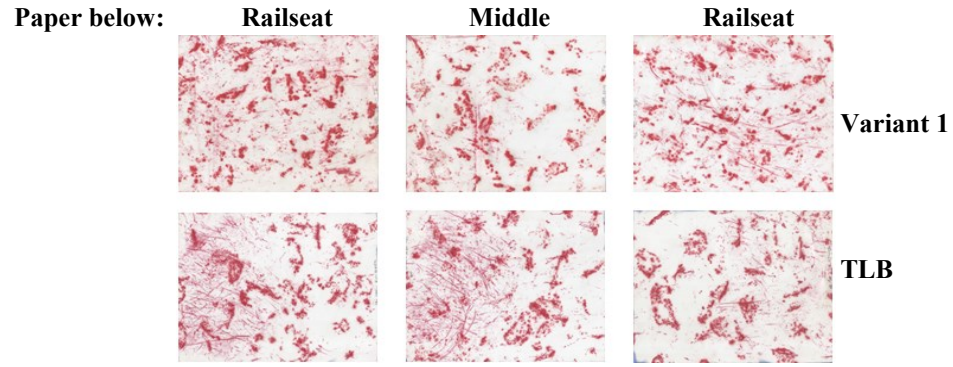

Figure 19: Contact areas recorded at the ballast/subgrade: mono-block concrete sleepers and TLB

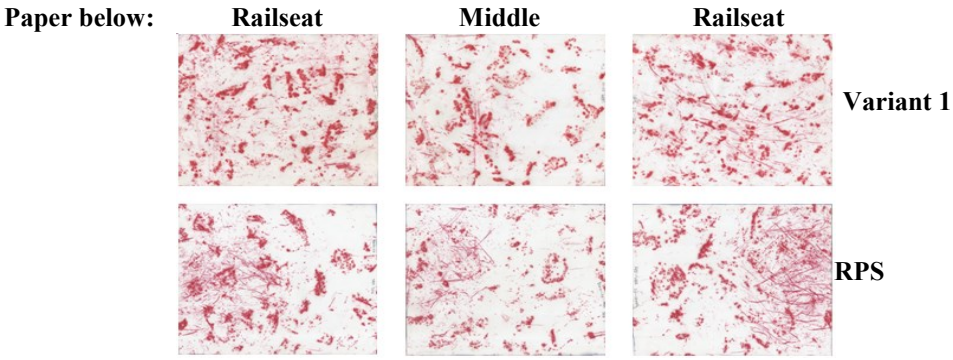

Figure 20: Contact areas recorded at the ballast/subgrade interface: mono-block concrete sleepers and re-profiled shoulder slopes

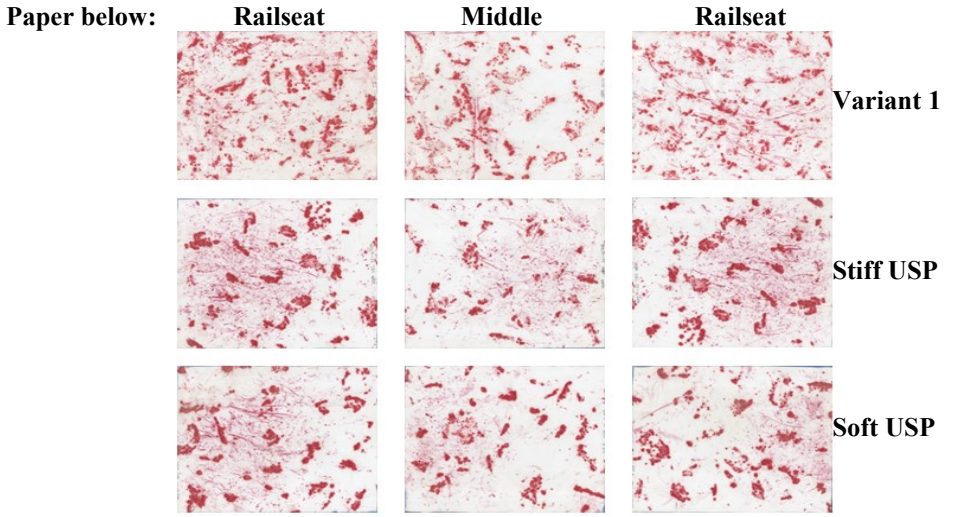

Figure 21: Contact areas recorded at the ballast/subgrade interface mono-block concrete sleeper and under sleeper pads

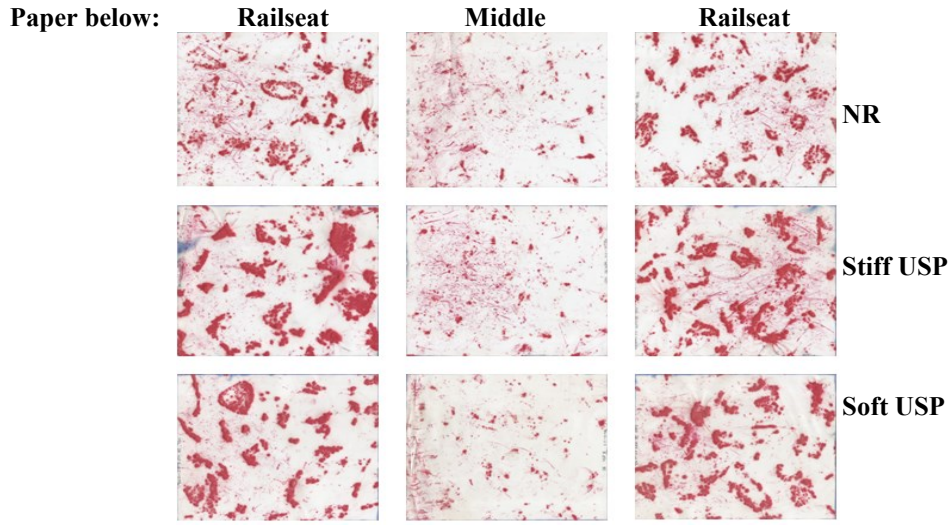

Figure 22: Contact areas recorded at the ballast/subgrade interface: twin-block concrete sleeper and under sleeper pads

In Figures 17 to 22, in general the paper below the railseats shows more red and more evidence of individual contacts migrating sideways from under the sleeper. It is also clear that the central paper below the twin-block sleeper has a much reduced contact area, which may be explained by the shape of the sleeper.

It was difficult to count the contact points at the ballast to rubber mat interface owing to the overlapping of red patches; however, because of the presence of the rubber mat there was less abrasion and lower maximum stresses at the contacts so that no wear holes appeared. Table 7 presents the measured contact areas.

Sleeper type	Test ID	Notes	% contact area per sleeper based on 2.5-10MPa rated paper (> 0.5 MPa)
Mono-block	Variant 1	Variant 1 grading	12.16
	Plastic	NR grading	15.05
	Timber		12.78
	Variant 2	↓ Increasing finer proportion	10.10
	Variant 3		16.88
	TLB	Two layered	12.50
	RPS	NR grading	10.96
	+ USP 1	Stiff	12.41
	+ USP 2	Soft	10.73
Twin-block	Baseline	NR grading	7.12
	Baseline		10.32
	+ USP 1	Stiff	16.29
	+ USP 2	Soft	12.88

Table 7. Proportions of the ballast/substrate interface area over which the contact pressure is at least 0.5MPa (pressure paper ranged of 2.5-10MPa)

The contact areas at the ballast/subgrade interface presented in Table 7 are substantially greater than the contact areas at the sleeper/ballast interface presented in Table 6. This is attributed to the particles pushing into the rubber to different degrees, giving a larger area of contact and a wider range of pressures with lower maximum values.

6 Discussion and further analysis

The data for the sleeper/ballast interface presented in Table 6 show considerable variability in terms of contacts and areas that cannot be explained solely by the differences in experimental set-up. This variability may arise because the pressure paper was not placed over the full sleeper base area so that extrapolating to the full area will introduce some uncertainty and because there will be some differences between repeat experiments anyway. Nonetheless, some important trends can be observed.

At the sleeper / ballast interface, the number of contacts for a mono-block sleeper on ballast with a grading similar to the NR standard (variant 1) was 147. This compares well with the range suggested by Shenton [5] of 100 to 200. For a twin-block sleeper, the value obtained was 243. The twin-block sleeper has a smaller base area so the increase compared to the mono-block sleeper is perhaps unexpected; however this higher number of contacts could be because the twin-block sleeper was tested to 4.5 million cycles (while the mono-block was to 3.0 million cycles). The result might also be explained by the twin-block sleeper having a smaller footprint and lower bending stiffness, which could be more effective in mobilising and retaining particle contacts over the loading history.

The material from which the sleeper is made also influences the number of contacts and the overall contact area. Plastic and timber mono-block sleepers showed 2 and 3 times greater numbers of contacts and 17 and 9 times larger percentage contact respectively than the concrete mono-block sleeper. This is thought to be primarily a result of the softer sleeper material allowing the ballast to indent into it and to encompass a larger number of contacts by pressing past the first contacting particles before then contacting others sitting lower down. Visually, more ballast particle indentations were observed at the end of testing in the plastic than in the timber sleeper soffit; this was reflected in the percentage area of contact, which was about double that of the wooden sleeper. Unusually for the plastic and timber sleepers, the number of contacts and the overall contact areas seem to show reverse trends while the wooden sleeper had a greater number of contacts the plastic sleeper had fewer contacts but spread over a greater area. This might have been because the plastic and wooden sleepers have differing bending stiffnesses hence different patterns of loading. This possibility is supported by the observation during testing that the plastic sleeper showed much greater bending beneath the railseats.

Changing the ballast grading by introducing finer materials was highly successful in increasing the number of contacts and percent contact. Ballast variant 3 increased the number of contacts by a factor of 5 (to 836) and the contact area by up to 3.5 times, while the modified TLB system with its finer layer of 10/20 material below

the sleeper increased the number of contacts nearly tenfold (to 1311) and the area of contact by slightly more than 3 times.

Re-profiling ballast shoulder slopes to 1V:2H increased the number of contacts by a factor of ~3, although, the total contact area was only increased by 11% compared with the baseline test. It is thought that this is a result of the re-profiled ballast shoulder being more effective in providing lateral restraint, hence preventing the sleeper / ballast contacts from moving as much thus additional stable contacts were developed as a result of the gradual vertical settlement of the sleeper. The less effective lateral restraint provided by shoulders with 1V:1H slopes meant that instead of new contacts being created, cyclic loading caused ballast particles to move laterally with the result that the fewer contacts present moved significantly over the course of the test.

The introduction of USPs 1 and 2 to the concrete mono-block sleeper soffit increased the number of contacts by between 2 and 3 times and the contact area by a factor of 9 and 6 respectively. As the USP type 2 was the softer it was expected to show an increased number of contacts and overall contact area over USP1; however while the number of contacts increased the contact area reduced. Again perhaps this reflects natural variation and experimental uncertainty from extrapolating the paper areas to the full sleeper.

The introduction of USPs at the twin-block concrete sleeper soffit increased the number of contacts by between 10% and 35% and the area of contact by a factor of 5.5 to 9. Again as for the mono-block this may be explained as a result of the more compliant material with the softer USPs giving the larger number and area of contacts. In this case, as expected, USP 2 showed both greater numbers of contacts and the greater percent contact.

Comparison of apparent contact stresses at the sleeper/ballast interface using a simplistic method of estimation (Table 6) illustrates that the average contact pressure can be drastically reduced by the use of plastic, timber, USPs and finer gradings in comparison to the basic configurations of either mono-block or twin-block concrete sleepers on standard NR ballast. In all cases, however, the average estimated contact stresses are much greater than that obtained from a simple averaging based on an effective railseat area using for example Equation 1. As an illustration the average contact stress based on equation 1 is less than 0.3% of that found based on the contact area for a mono-block concrete sleeper with ballast variant 1 after 3 million load cycles.

In the case of the data evaluated in this paper D_{90} is generally close to 49 mm (Table 3) and D_{50} is known. These values can be used together with Equation 3 to determine the coefficients m and C and any value of D_A, D_B to D_N desired. If a range of D_{50} values are chosen an estimate of the potential number of contacts available can be made using Equation 5 and plotted against the variation in D_{50}. The calculated potentially available number of contacts can then be compared with those measured as shown in Figure 23. In Figure 23, 5 particle sizes corresponding to D_{90}, D_{70}, D_{50}, D_{30}, and D_{10} have been evaluated to produce the curves for potentially available contacts.

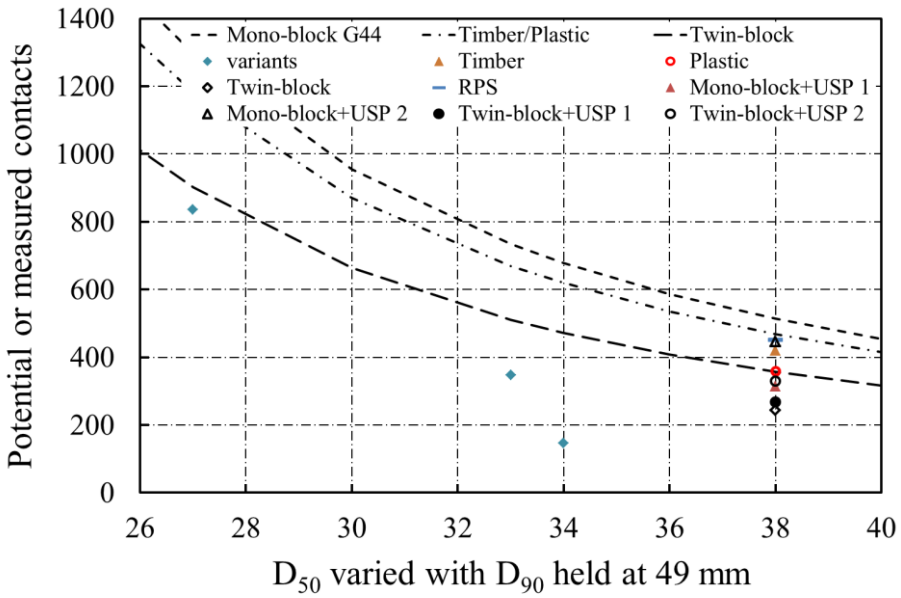

Figure 23. Number of contacts versus D_{50}: measurements and estimates (dashed lines)

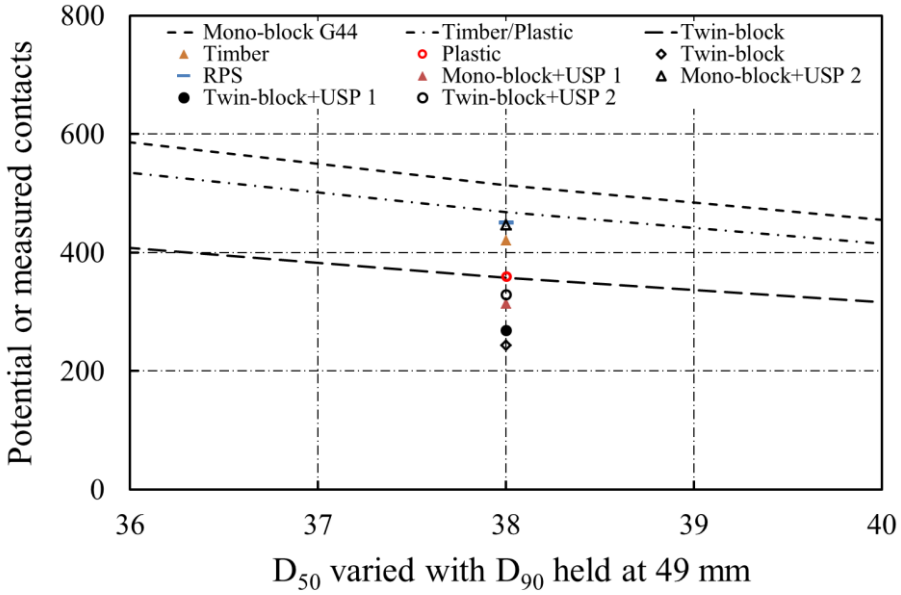

Figure 24. Number of contacts versus changing D_{50} for a log linear PSD and fixed D_{90} of 49 mm: measurements and estimates (dashed lines)

Most of the combinations tested used standard NR ballast and hence the majority of data points plot along a vertical line where D_{50} = 38 mm. Figure 24 shows a close up of this region.

Figures 23 and 24 show that the gradings tested all have a lower number of contacts than the estimated potential number of contacts available. The difference between the measured and the potential number of contacts can be viewed as an indication of the quality of the surface preparation achieved and/or the benefit from USPs, wood, plastic compared to concrete. Table 8 compares the measured and calculated potential contacts and shows a parameter termed the “contact efficiency” which is

defined as the measured number of contacts divided by the calculated estimate of potentially available contacts. For completeness the potential number of contacts estimated for a mono-block sleeper on NR ballast is included, although no measurements are available for this it can be observed that the number of potential contacts for NR ballast is about 25% less than those estimated for variant 1.

Sleeper type	Test	Measured contacts	Potential contacts	Contact Efficiency (%)
Mono-block	NR	N/A	513	N/A
	Variant 1	147	679	21.6%
	Variant 2	347	735	47.2%
	Variant 3	836	1297	64.5%
	Plastic	360	468	76.9%
	Timber	420	468	89.7%
	RPS	451	513	87.9%
	+ USP 1	314	513	61.2%
	+ USP 2	447	513	87.1%
Twin-block	NR	243	357	68.1%
	+ USP 1	268	357	75.1%
	+ USP 2	329	357	92.2%
Mono-block	TLB	1311	2917	44.9%

Table 8. Measured and potential contacts

Table 8 also includes the test on 10/20 aggregate (the TLB test) although this test was not plotted on the graphs owing to the much different D_{90} value.

Comparing the contact efficiencies (Table 8) and the measured contacts shows that while the use of finer gradings can increase the absolute number of contacts mobilised there are more effective ways to mobilise greater proportions of the potentially available contacts. The use of timber sleepers, a shallower ballast shoulder, and the use of USP2 all mobilise more than 80% of the estimate of potentially available contacts.

At the bottom of the ballast layer at the interface with the subgrade, the percentage areas of contact were much larger beneath the railseats than in the middle of the sleeper (Figures 19-21). This may be a result of the ballast beneath the railseats migrating sideways from underneath the track. The contact area is then overestimated, being in effect the sum of all contact areas during the test. Overall the range of contact areas was between 7% and 17% for contact pressures greater than 0.5MPa but there seems to be a great deal of noise in the data. It appears that by the time the stresses have transferred through the ballast layer there is much less variation at the ballast/subgrade interface, almost regardless of the type of ballast or sleeper used. However, while trends are less clear it is perhaps worth noting that the finest ballast grading (variant 3) showed the highest contact area at the subgrade and the lowest contact area at the subgrade was given by the twin-block sleeper on NR ballast.

5 Conclusions

Pressure paper can be used to obtain a record of contact locations between ballast particles and the sleeper soffit or the subgrade, over a number of load cycles. However, not all of the indicated contacts would necessarily have been active at the same time.

The tests reported in this paper have quantified and demonstrated the potential for different ballast/sleeper combinations to improve the number and area of contacts at the sleeper to ballast interface and to some extent to modify these parameters at the ballast to subgrade interface. The changes in contact area imply large changes in the contact stresses. Values are presented in the preceding sections, however, in general the key findings can be summarised as follows:

For the sleeper to ballast interface, increases in the number and area of contacts can be achieved by:

- Finer ballast gradations, including the use of a layer of finer material beneath the sleeper
- USPs with softer USPs producing the greatest increase
- Using lower stiffness sleeper materials such as wooden or plastic sleepers

When considered in terms of mobilising larger proportions of potentially available contacts the most effective interventions are the use of timber sleepers, a shallower ballast shoulder, and the use of softer USPs (USP2).

Perhaps most significantly it has been shown that under normal conditions the sleeper to ballast contact area is less than 1% of the sleeper footprint and the contact stresses that this implies are orders of magnitude greater than those calculated from the simplistic pressure distributions commonly used. Thus the contact behaviour cannot be understood without considering the discrete nature of the contacts at the interface. Larger numbers of contacts and larger contact areas imply lower stresses and greater homogeneity of load transfer from the sleeper to the ballast. This is desirable as it will lead to less ballast breakage and a more uniform response to train loading along the sleeper base and along the track length.

At the ballast/subgrade interface the different sleeper and ballast combinations tested showed much less influence on the contact area and it was difficult to identify clear trends due to natural variation in the data. However, most notably the twin-block sleeper on NR ballast showed the smallest contact area while the concrete mono-block sleeper on the finest ballast gradation showed the highest contact area.

Acknowledgements

This research was funded by the UK Engineering and Physical Sciences Research Council (EPSRC) as part of the TRACK21 project (grant: EP/H044949). Tiflex Ltd supplied the under sleeper pads.

References

[1] Zakeri, J. A. & Sadeghi, J.,"Field investigation on load distribution and deflections of railway track sleepers", Journal of Mechanical Science and Technology, 21**,** 1948-1956, 2007.

[2] Esveld, C, "Modern railway track", MRT Productions, 2001.

[3] AREMA, "Economic of railway engineering and operations: Manual for railway engineering: Systems management: chapter 16, 2003.

[4] British Standard Institution, "British Standard Institution BS EN 13230-2:2009 Railway applications -track - concrete sleepers and bearers: Part 2: Prestressed mono-block sleepers", British Standard Institution, 2009.

[5] Shenton, M. J, "Deformation of railway ballast under repeated loading condition", in "Proceeding of Railroad Track Mechanics and Technology", Kerr, A.D, (Editor), Princeton University, 1978.

[6] Le Pen, L. M., "Track behaviour: The importance of the sleeper to ballast interface", Theses of Doctor of Philosophy, University of Southampton, 2008.

[7] Le Pen, L. M, & Powrie, W, "Contribution of base, crib, and shoulder ballast to the lateral sliding resistance of railway track: a geotechnical perspective", in "Proceedings of the Institution of Mechanical Engineers Part F-Journal of Rail and Rapid Transit", 225**,** 113-128, 2011.

[8] Raymond, G. P, "Analysis of track support and determination of track modulus", Journal of Transportation Research Record", 1022**,** 80-90, 1985.

[9] Timoshenko, S., "Methods of analysis of statical and dynamical stresses in rails", in "Proceedings Second International Congress of Applied Mechanics", 407-418, Zurich, 1927.

[10] A J P Automotive Ltd, "Pressure measurement film prescale", 2011.

[11] Fuji Film, "Fuji film prescale pressure measurement film", Available: http://www.fujifilm.com/products/prescale/prescalefilm/, 2013.

[12] Andussies, R, "Pressure measurement film analysing", 2011.

[13] MathWorks,"MathWorks: Accelerating the pace of Engineering and Science", [Online]. Available: www.mathworks.co.uk [Accessed 28th May 2014], 2014.

[14] Network Rail, "Network Rail RT/CE/S/006: Railtrack line specification: track ballast and stone-blower aggregate", Railtrack House, Euston Square, London NWI 2EE: Railtrack Plc, 2000.

[15] British Standard Institution, "British Standard Institution PD 6682-2:2009 Published Document Aggregates: Part 2: Aggregates for bituminous mixtures and surface treatments for roads, airfields and other trafficked areas-Guidance on the use of BS EN 13043", British Standard Institution, 2009.

[16] Ionescu, D,"Evaluation of the engineering behaviour of railway ballast", Theses of Doctor of Philosophy, University of Wollongong, 2004.

[17] Selig, E. T., Parsons, B. K. & Cole, B. E, "Drainage of railway ballast", in "Proceeding of the 5th International Heavy Haul Railway Conference". Beijing, China, 1993.

[18] Indraratna, B, & Salim, W, "Mechanics of ballasted rail tracks : a geotechnical perspective", Taylor & Francis, London, 2005.

[19] UIC, "UIC Leaflet 713-1R: Recommendations for the use of under sleeper pads-USP", GROUP, T. E, (Editor.), 2008.
[20] UIC, "UIC Project: Under sleeper pads- Semelles sous traverses-Schwellenbesohlungen", 4th ed. Vienna, 2009.
[21] Tiflex Ltd, "TRACKELAST specialist rail solutions: the high performance solution", Available: http://www.tiflex.co.uk/downloads/TFX-B-TRACKELAST-10092012_A4.pdf [Accessed 23/05/2013 2013].
[22] Auer, R, Potvin, R, Godart, P, & Schmitt, L, "Track systems supplement: under sleeper pads in track-the UIC project", European Railway Review, 2013.
[23] British Standard Institution, "British Standard Institution BS EN 13230-3:2009 Railway Applications -track - concrete sleepers and bearers: Part 3: twin-block reinforced sleepers" British Standard Institution, 2009.
[24] Anderson, W. F., & Key, A. J, "Model testing of two-layer railway track ballast", Journal of Geotechnical and Geoenvironmental Engineering, 126, 317-323, 2000.
[25] Fair, P. I. & Anderson, W. F, "Railway track maintenance using the stone blower", in "Proceeding of The Institution of Civil Engineers", Transport 156**,** 155-167, 2003.
[26] Fair, P. I,"The Geotechnical behaviour of ballast materials for railway track maintenance", Thesis of Doctor of Philosophy, University of Sheffield, 2003.
[27] Claisse, P., Keedwell, M, & Calla, C, "Tests on a two-layered ballast system", in "Proceeding of the Institution of Civil Engineers", Transport 156, 93-101, 2003.
[28] Claisse, P. & Calla, C, "Rail ballast: conclusions from a historical perspective", in "Proceedings of the Institution of Civil Engineers", Transport, 159**,** 69-74, 2006.
[29] Quinn, A. D., Hayward, M., Baker, C. J., Schmid, F., Priest, J. A. & Powrie, W., "A full-scale experimental and modelling study of ballast flight under high speed trains", in "Proceedings of the Institution of Mechanical Engineers", Part F: Journal of Rail and Rapid Transit, 61-74, 2009.
[30] Marx, L. & Mobmann, D, "DB Manual work procedures for permanent way maintenance", Bahn Fachverlag, 2012.
[31] Country Regional Network., "Engineering standard track: CRN CS 240: Ballast, 2013.
[32] AREMA, "American railway engineering and maintenance-of-way association: chapter 1: roadway and ballast: ballast. 2012.
[33] UIC, "UIC Code 719R Earthworks and trackbed for railway lines", 2008.
[34] Abadi, T, "Effect of sleeper and ballast interventions on rail track performance". Thesis of Doctor of Philosophy, Faculty of Engineering and the Environment, University of Southampton, Southampton, U.K, 2015.